PHILOSOPHICAL TRANSACTIONS B

*Phil. Trans. R. Soc. B.*
doi:10.1098/not yet assigned

# A resilience sensing system for the biosphere

**Timothy M. Lenton[1*], Joshua E. Buxton[1], David I. Armstrong McKay[1,2], Jesse F. Abrams[1,3], Chris A. Boulton[1], Kirsten Lees[1,4], Thomas W. R. Powell[1], Niklas Boers[1,5,6], Andrew M. Cunliffe[1], Vasilis Dakos[7]**

*[1]Global Systems Institute, University of Exeter, Exeter EX4 4QE, UK*
*[2]Stockholm Resilience Centre, Stockholm University, Stockholm, Sweden*
*[3]Institute for Data Science and Artificial Intelligence, University of Exeter, Exeter EX4 4QF, UK*
*[4]Environmental Sustainability Research Centre, University of Derby, Derby DE22 1GB, UK*
*[5]School of Engineering & Design, Earth System Modelling, Technical University of Munich, Munich, Germany*
*[6]Potsdam Institute for Climate Impact Research, Potsdam, Germany*
*[7]ISEM, University of Montpellier, CNRS, EPHE, IRD, Montpellier, France*

*ORCID: TML: 0000-0002-6725-7498; JEB: 0000-0001-9664-0368; DIAM: 0000-0002-0020-7461; JFA: 0000-0003-0411-8519; CAB: 0000-0001-7836-9391; KL: 0000-0001-9254-2103; AMC: 0000-0002-8346-4278; VD: 0000-0001-8862-718X*

**Keywords:** Resilience, recovery rate, biosphere, ecosystems, remote sensing, climate change

# Main Text

## Summary

We are in a climate and ecological emergency, where climate change and direct anthropogenic interference with the biosphere are risking abrupt and/or irreversible changes that threaten our life-support systems. Efforts are underway to increase the resilience of some ecosystems that are under threat, yet collective awareness and action are modest at best. Here we highlight the potential for a biosphere resilience sensing system to make it easier to see where things are going wrong, and to see whether deliberate efforts to make things better are working. We focus on global resilience sensing of the terrestrial biosphere at high spatial and temporal resolution through satellite remote sensing, utilising the generic mathematical behaviour of complex systems – loss of resilience corresponds to slower recovery from perturbations, gain of resilience equates to faster recovery. We consider what subset of biosphere resilience remote sensing can monitor, critically reviewing existing studies. Then we present illustrative, global results for vegetation resilience and trends in resilience over the last 20 years, from both satellite data and model simulations. We close by discussing how resilience sensing nested across global, biome-ecoregion, and local ecosystem scales, could aid management and governance at these different scales, and identify priorities for further work.

## 1. Introduction

Faced with a climate and ecological emergency, we need to be able to sense where things are going wrong in our life-support systems, to have any chance of correcting our mistakes, and we need to be able to sense where they are going right to know what to seek to replicate [1]. Establishing changes in the mean state of ecosystems and the biosphere are important to this, but they do not tell the whole story. A complex system may lose stability without its mean state changing, or the mean state may change without any underlying change in stability. Hence there has been half a century of growing scientific interest in the *resilience* of ecosystems [2] and the biosphere [3] – meaning here the self-regulation capacity of a system to recover from perturbations. Currently there is growing concern that self-regulation may be breaking down in some ecosystems and biomes, in response to climate change and direct human interference, potentially

*Author for correspondence (t.m.lenton@exeter.ac.uk).

leading to abrupt transitions or 'tipping points' [4, 5]. Consequently, there is a widespread stated desire from policymakers and other societal actors to increase the resilience of (social-) ecological systems in the face of global change stressors. In response, a growing number of scientific studies are seeking to monitor the resilience of different (social-) ecological systems. However, they are using disparate definitions of resilience and methods of quantifying it. Bringing resilience sensing efforts together in a consistent, global approach could be a valuable tool to help navigate the near future. A resilience sensing system for the biosphere could help quantify the resilience of different (social-) ecological systems, how it is changing, and whether societal efforts (e.g. policy interventions) to increase the resilience of particular systems are having the desired effect or not. It could raise collective awareness of the growing climate and ecological emergency, by 'bringing to life' the dynamical response of the biosphere and gathering that complex spatial and temporal information visually in one place. Furthermore, if 'users' of resilience sensing information responded by changing their actions that impact upon resilience, this would amount to a new type of self-aware feedback within ecosystems and the biosphere [1].

A resilience sensing system clearly needs a consistent underlying definition of resilience and methods of quantifying it. To be useful – scientifically and practically – it also needs to be clear about the resilience of what to what that it seeks to monitor [6]. Here we focus on land-surface ecosystems, especially their vegetation component, and what remotely sensed data can reveal about terrestrial biosphere resilience. We consider resilience to a range of perturbations, including climate variability (e.g. drought), disturbance (e.g. fires), and direct human interference (e.g. deforestation). Assessing how resilience to perturbations changes over time, or with respect to environmental or disturbance gradients, can in turn enable an assessment of how resilience depends on longer-term drivers, including climate change or land-use change. Focusing on remotely-sensing resilience is timely thanks to the development of: (a) an established mathematical framework and algorithms to detect changes in resilience; (b) sufficiently long remotely-sensed products (e.g. from Landsat, MODIS) to apply data-hungry resilience sensing methods; (c) advances in remote sensing sensitivity and capacity that can provide global coverage at ever finer temporal and spatial resolution, and; (d) more efficient ways to handle the massive volume of data generated (e.g. through portals such as Google Earth Engine and the Microsoft Planetary Computer).

Our aim in this paper is to outline key elements of a resilience sensing system for the terrestrial biosphere, which spans a range of scales from local ecosystems to global vegetation. We discuss the state of research in the field, critically reviewing existing attempts to extract measures of terrestrial ecosystem resilience from remotely-sensed data products (Table 1). We synthesise this with examples of analyses from our own prototype resilience-sensing system at biosphere-to-biome scales. This effort is important because currently we lack a global, quantitative overview of which ecosystems are least resilient, which are losing resilience fastest, and whether localised efforts to increase resilience are working. The paper is novel in bringing together a synthesis of many disparate studies towards designing a biosphere resilience sensing system, and outlining its potential benefits. The structure is as follows: We start by clarifying our chosen definition of resilience and how to measure it. Then we consider what subset of biosphere resilience remote sensing allows us to measure. We illustrate how resilience sensing can be nested across scales from global to local. Then we outline how it could aid ecosystem governance and management at these different scales, and identify priorities for further work.

## 2. Defining and measuring resilience

A resilience sensing system requires a clear underlying definition of resilience and how to measure it. The concept of 'resilience' has a long history in ecology, where different authors have adopted different definitions [2, 7-9]. Recent, more widespread use of 'resilience' in diverse contexts, including normatively (as a desired feature), has led to yet more disparate meanings [10, 11]. Furthermore, existing efforts to quantify 'resilience' from remotely sensed data use different definitions of resilience and different ways of measuring it (Table 1).

We focus on resilience as the capacity of a system to recover from perturbations, which is a characteristic property of living organisms, and of a much broader class of self-regulating systems, including aspects of the biosphere as a whole [12]. Hence, we favour a simple, theoretically grounded definition of resilience, based on dynamical systems theory (Box 1). This equates resilience with the rate at which a system recovers from perturbations [7], which can be quantified as the magnitude of the leading (negative) eigenvalue, reflecting the strength of negative feedbacks restoring a system back towards an initial attractor after perturbation. Some authors refer to this recovery rate more restrictively as 'engineering resilience' [13] or rename it 'elasticity' [8]. Ecologists usually distinguish recovery rate from 'resistance', which they relate to the inverse of the magnitude of a system's response to perturbation [7]. However, the magnitude of response to perturbation also depends (in part) on the strength of negative feedback in a system (Box 1). Hence, resistance usually changes together with resilience, when the strength of negative feedbacks governing a dynamical system changes – as resilience goes up, variance goes down (and *vice versa*) (Box 1; Eq. (2)).

The most intuitive way to measure resilience is to wait for a system to be perturbed and measure how fast it recovers [14, 15]. Ecosystems are frequently subject to perturbations that affect their functioning. For relatively small perturbations,

recovery should follow an exponential decay from the initial perturbation back to equilibrium, and recovery rate should be independent of perturbation size, following linear stability analysis (Box 1, Eq. (3)). In such cases, one can estimate recovery rate (dimensions $[T]^{-1}$) by linearly regressing the logarithm of the data onto the decay interval. This requires that sampling of the system is more frequent than the inverse of the recovery rate. Other studies try to measure 'resilience' by measuring 'recovery time' as the time to return from the peak of a perturbation (close) to a presumed baseline equilibrium [16-18]. This can be used to compare response to the same event of uniform magnitude, e.g. a specific drought [17]. However, when comparing responses across events, for a fixed recovery rate (i.e. fixed resilience) a larger perturbation will take a longer time to recover to a given distance from a presumed equilibrium. Yet further studies try to deal with this by measuring 'resilience' as peak response to perturbation ('event size' or 'maximum stress') divided by 'recovery time' [19-21]. However, this assumes a linear (not exponential) recovery from perturbation, and introduces the dimensions of whatever is the state variable, losing generality. All these approaches require a measure of the equilibrium state, which in ecosystems usually changes with the seasons as well as any slower changes in forcing.

**Box 1.** Resilience theory and leading indicators.

Let us assume (preferably based on observations) that some state variable of a dynamical system, $x$, tends to recover from some range of perturbations back towards a previous state. Mathematically this suggests it may exhibit an 'attractor', which in one dimension ($x$) can be assumed to be a stable fixed point (i.e., an equilibrium state) $x^*$ around which the dynamics takes place. There may be other attractors, and boundaries to the present attractor beyond which recovery will not occur. That can all be described with a potential function, $U(x)$, often sketched as a valley (sometimes with other hilltops and valleys), with the current state of the system ($x$) represented as a ball, which tends to roll back to the bottom of the valley ($x^*$). The system may be subject to known perturbations, or more generally, to noise. For simplicity, let us consider additive white noise $\eta$ with standard deviation $\sigma$. The corresponding dynamics are described by:

$$\frac{dx(t)}{dt} = -U'\big(x(t)\big) + \eta(t) \quad (1)$$

Close to the fixed point ($x^*$) the potential function $U$ can be approximated by a quadratic function with minimum at $x^*$, such that for some parameter $\lambda < 0$, $U(x) \sim \frac{-\lambda}{2}x^2$. $\lambda$ (the leading eigenvalue) is the recovery rate from perturbations and a direct measure of the strength of negative feedback. The closer that $\lambda$ is to zero, the less stable is the fixed point. At $\lambda = 0$ stability is lost. Discretizing the dynamics into timesteps $\Delta t$ gives an autoregressive process for which the variance and the autocorrelation function at $n$ timesteps $\alpha(n)$ are known analytically:

$$var(\Delta x) = \frac{\sigma^2}{1-e^{2\lambda\Delta t}} \sim -\frac{\sigma^2}{2\lambda\Delta t} \quad (2)$$

$$\alpha(n) = e^{n\lambda\Delta t} \quad (3)$$

Where stability increases, and thus resilience is being gained ($\lambda$ is getting more negative), lag-1 autocorrelation ($\alpha(1)$ or 'AR(1)') and variance will decline. When resilience is being lost ($\lambda$ is approaching zero from below), both AR(1) and variance increase. These are the classical early warning indicators of 'critical slowing down' prior to a transition to an alternative attractor [5, 22-25]. However, whether or not an alternative attractor is known to exist, we can still quantify resilience (the strength of restoring negative feedback). Variance also depends on the magnitude of perturbation; here, $\sigma$, the amplitude of the noise. AR(1) is independent of $\sigma$, hence should be a more robust, generic indicator of resilience than variance. However, if we can diagnose the magnitude of perturbing variability (here $\sigma$) and any changes in that, this can be controlled for, and changes in variance of response can be used to diagnose resilience.

Where perturbations of a system are continuous or not well characterised, but it remains close to equilibrium and a sufficiently long time series is available, the recovery rate can be extracted from the temporal autocorrelation (AR(1); denoted $\alpha(1)$ in Box 1, Eq. (3)). Attributing changes in variance and autocorrelation to a change in stability assumes stationarity of the data. The seasonal cycle and any long-term trends therefore need to be carefully removed before estimating both indicators. Sufficient, evenly spaced data are also required to reliably estimate AR(1) (e.g. ~50 data points for monthly data in the presence of a seasonal cycle [26]). Variance depends on perturbation amplitude as well as recovery rate hence to isolate the recovery rate, perturbation amplitude must also be estimated (Box 1; Eq. (2)). In systems where the noise of perturbations is not additive (as in Box 1) but multiplicative – i.e. its effect depends on the state of the system – variance can become decoupled from recovery rate [27]. As well as AR(1), the whole autocorrelation function can be used to deduce resilience. De-trended Fluctuation Analysis (DFA) considers how correlations decay as a function of time lag, extracting a power law exponent which describes that decay (essentially, correlation increases further away in time as resilience is lost). This is equivalent to a spectral analysis, where loss of resilience corresponds to reddening of the response spectrum. For the approach to particular types of bifurcation, higher-order terms (neglected in the linearization of Box 1) and additional statistical moments can be informative of the type of bifurcation being approached, as well as its proximity [28]. Deep learning can utilise these to distinguish the type of

tipping point being approached and provide improved early warning [29]. For example, skewness increases prior to a saddle-node bifurcation, with the data skewing towards the new state. A toolbox of associated algorithms is available [30].

To assess whether resilience of a system is changing over time, we first need to consider the rate at which a system is being forced (e.g. by climate change) in comparison to its recovery rate (the intrinsic timescale of the system). For the system to remain close to equilibrium, forcing must be considerably slower than recovery rate. For e.g. climate change and ecosystems, this will generally be the case, but for more rapid changes in e.g. land-use, it may not be. Then to pick up the effect of changes in forcing upon resilience we need to monitor the system over the forcing timescale, which may demand long records. Once confident in a separation of timescales, the methods described above can be repeatedly applied over time. If the same ecosystem is perturbed multiple times, changes in recovery rate may become detectable, e.g. recovery of tidal marshes from inundation events [31, 32], or recovery of forest from disturbance [33]. Statistical measures such as AR(1) and variance can be recalculated in a sliding window moving through a longer dataset and trends indicated using e.g. Kendall's tau rank correlation coefficient ($\tau$). Then as a sensitivity analysis, the bandwidth used for e.g. Gaussian de-trending and the sliding window length can be varied [30].

For relatively 'slow' systems where the length of time we have been monitoring them (e.g. via remote sensing) is sufficient to quantify their resilience but not to diagnose changes in resilience, a space-for-time substitution can be made to look over space for variations in temporal indicators that correlate with particular environmental driving variables. For example, AR(1) of tropical forest greenness (NDVI) increases sharply below a critical threshold in mean annual precipitation [34], consistent with evidence of multiple stable states for tropical vegetation depending on rainfall [35, 36].

Some ecosystems lack sufficient temporal data. However, for systems that are coupled across space with associated spatial feedbacks, equivalent spatial indicators of resilience exist, including spatial correlation, spatial variance, spatial skewness, and spatial frequency spectra [37, 38] – a gain with a toolbox of algorithms available [38]. Despite the spatial richness of remotely sensed data, relatively few studies have estimated spatial resilience indicators (Table 1) – notable exceptions being for vegetation data along rainfall gradients in the grassland–savannah-woodland systems of the Congo, Australia, and Serengeti [39, 40]. Where sufficient spatial and temporal data are available, a resilience indicator combining spatial and temporal correlations can be more reliable, and forewarn of global as well as local bifurcations [41]. Spatial feedbacks are not necessarily dominantly negative in sign, and they may generate irregular or regular vegetation patterns. In the case of regular ('Turing') patterns, these are a spatial manifestation of a balance of positive and negative feedbacks operating on different length scales, they may undergo global bifurcations, and the nature of the pattern itself may carry resilience information [42]. In systems that can be characterised as networks, network-based indicators of resilience are also available [43, 44].

To test hypotheses of changing resilience it is essential to have appropriate null models. Repeatedly bootstrapping temporal data to destroy their memory can provide a null model distribution for tests on temporal indicators [45, 46], but it is better to preserve the overall variance and autocorrelation of the underlying time series, for example by randomizing phases in Fourier space [47]. Bootstrapping spatial data works for spatial correlation tests, but not for e.g. spatial variance, for which alternative null model approaches are available [38]. However, few remote sensing studies (Table 1) test against a null model to establish whether signals are statistically significant/robust – a notable exception being a lake study using an autoregressive moving average (ARMA) null model [48].

Some studies (Table 1) purporting to measure 'resilience' are unrelated to recovery rate – in particular those considering persistence of trends in NDVI [49-52]. These trends are estimated to have lifetimes of e.g. ~5–17 y [49], whereas for the same biome, the correlation timescales of NDVI are estimated to be ~0.1–1.4 y [53-55]. Therefore, perturbations decay (much) faster than trends persist. Indeed studies using annual [49, 52] or coarser [51] resolution data will be unable to resolve recovery timescale. Instead, persistent NDVI trends could reflect e.g. steady forest growth, but likely also respond to well-known decadal climate variability.

Other studies (Table 1) combine statistical indicators, including AR(1) and variance, into a composite indicator [56, 57], but generally without clear justification for their relative weighting, and with the drawbacks of e.g. merging aspects of resilience and resistance, and double-counting the effects of recovery rate. Particularly problematic is where opposing signals of 'critical speeding up' (a questionable notion) and critical slowing down (well-established) are both considered as indicators of resilience loss in a single composite indicator [57].

## 3. Remotely sensing resilience

Remote sensing using satellite instruments provides an opportunity to globally monitor the resilience of terrestrial ecosystems over large spatial scales, but also poses challenges. Relatively short records, noisy data, and gaps (e.g. due to

cloud cover, instrument failure) are familiar constraints [58], which obfuscate different statistical resilience indicators to varying degrees [59]. To understand what aspects of resilience remote sensing can capture key questions are: What biosphere state variables reflect a system's resilience i.e. are governed by negative feedback? What remote sensing data products (if any) can provide an indirect proxy for these state variables, and how good/bad a proxy? What are the relevant temporal and spatial scales of the system and the monitoring (and do they overlap)?

Evolution by natural selection tends to optimise survival and/or reproduction of organisms, including adaptively refining their physiological self-regulation mechanisms. For example, plants self-regulate photosynthetic activity and respiration, having evolved to maximise net primary production subject to environmental constraints (including avoiding damage from excess wind or radiation, and in the case of deciduous plants avoiding costly maintenance of leaves in winter or in drought). Hyperspectral indices and fluorescence are sensitive to both short-term changes in photosynthesis and interacting photo-protective mechanisms, and are often highly variable. The normalised difference vegetation index (NDVI) is a simple measure of greenness related to chlorophyll, which relates (imperfectly) to gross primary production. However, it is also sensitive to changes in species composition, vegetation health, and vegetation distribution [58]. Furthermore, it saturates in densely vegetated settings (e.g. forests). The enhanced vegetation index (EVI) has less saturation in such settings, but both NDVI and EVI have issues in drylands with lots of bare soil, where Soil Adjusted Indices (SAVI and MSAVI) retrieve more vegetation signal. Models of Net or Gross Primary Productivity (NPP or GPP) often use vegetation indices in combination with other datasets [60], whilst models of Leaf Area Index (LAI) are derived from reflectance data [61]. All these optical indices can change on relatively fast timescales as plants respond to seasonal change in light, temperature and water availability. Thus, for fast-responding vegetation (e.g. annual grasses), they may reflect whole-plant resilience.

However, for slower-growing, larger, perennial plants – especially trees – the fluctuating greenness of leaves does not fully capture whole-plant resilience. Rather, these plants regulate their biomass, which is predominantly woody material. Microwave backscatter and related indices such as Vegetation Optical Depth (VOD) can be sensitive to aboveground biomass but also soil and vegetation moisture content, and surface and canopy roughness. LiDAR can characterise forest structure and thus biomass, but has relatively short duration missions, limited spatial coverage, and is insensitive at low biomass levels. Combining independent data products [62, 63] may reveal more about ecosystem resilience. For example, combining an optical vegetation index (e.g. NDVI) and a microwave-based index (e.g. VOD) may give better monitoring of fluctuations in aboveground biomass and associated resilience [63]. Most published attempts to monitor resilience (Table 1) focus on NDVI, with some using EVI, modelled GPP or LAI (Table 1). A couple of studies use VOD as a proxy for tropical forest biomass [34, 64] which better captures changes in forest cover than NDVI [64]. However, in general there needs to be greater consideration of which indexes are appropriate for monitoring resilience of the vegetation in question.

Spatial resolution poses another fundamental issue. Individual remote sensing pixels in satellite products are rarely fine enough resolution to capture individual plants hence most data products sample aggregated behaviour. The implicit working hypothesis must be that nearby plants exhibit correlated resilience responses to larger-scale drivers (such as climate variability). However, pixels may mix differing resilience responses of different plants to the same driver, e.g. canopy trees and underlying grass in savannah responding differently to fire. Furthermore, pixels are typically aggregated to larger spatial scales, ranging up to ~1–10 km, before performing resilience analysis (Table 1). This amplifies the potential problem of different vegetation types or different ecosystems within a grid cell exhibiting different resilience responses. The problem will be less acute in more spatially uniform systems, e.g. the Amazon rainforest. However, for highly heterogeneous, densely human populated landscapes, e.g. Italy [50], it is an issue.

At ecosystem scale there are multiple feedback loops involving multiple species affecting shared state variables such as fractional tree coverage, or resource pools e.g. nutrients or soil water, which can exhibit system-level resilience. The presence and strength of negative feedback on such variables – i.e. their resilience – is widely recognised, but not generally understood as refined by natural selection – although see [65]. As such, we may expect regulation to be weaker than for the productivity or biomass in individual plants, but nonetheless important to measure. Only some ecosystem variables are accessible to current remote sensing, e.g., ground-penetrating synthetic aperture radar (SAR) can provide a reliable proxy for the water table depth in peatlands, which is regulated by the ability of the bog to retain water, as well as incoming rainfall [17]. Multi-modality of remotely-sensed tree cover with respect to climate and other drivers has been used to estimate alternative ecosystem stable states and spatially locate them [35, 36, 66-68]. However, coarse spatial and temporal resolution limits its potential for extracting spatial or temporal resilience metrics.

At the biome scale there are instances of large-scale feedback acting to regulate biome state, notably the Amazon rainforest recycling (and redirecting) its own rainfall [69], and boreal forests warming their winter regional climate [70]. Associated loss of resilience could end in large-scale forest dieback [5]. For the Amazon, modelling suggests that the aggregate impact of the forest on atmospheric $CO_2$ variability could provide a (remotely sensed) proxy of resilience [71]. Specifically, fluctuations in forest carbon storage and hence atmospheric $CO_2$ become more sensitive to temperature anomalies as the forest loses resilience [71].

At the biosphere scale, the existence of negative feedbacks is now widely recognised – despite perennial debate over whether it can have an evolutionary explanation [12]. A key example are the land and ocean carbon sinks, which together remove ~55% of anthropogenic $CO_2$ emissions [72] and thus also damp global warming. Remote sensing of spatial and temporal fluctuations in atmospheric $CO_2$, make the recovery rate of $CO_2$ fluctuations a potential target for biosphere resilience sensing, which might be extended to methane ($CH_4$) and other trace gases.

A biosphere resilience sensing system should ideally span and connect these different scales from local to global in a single software platform, whereas existing studies are scattered across spatial scales (Table 1). Taking a top-down approach allows one to consider the whole system and look for large-scale patterns before trying to isolate the most acute problems [73]. That said human agency to improve biosphere resilience is often greatest at smaller ecological scales, so striving to resolve what is happening to resilience at those scales is essential.

## 4. Results across scales

Here we synthesise new analyses and existing results (Table 1) regarding terrestrial biosphere resilience across scales. Biosphere scale distinctions are fuzzy, but we loosely group them into global, biome-ecoregion, and ecosystem scale studies. We start by trying to get a global picture of biosphere resilience and its variation across space, and over recent time – to begin to see if patterns emerge.

## (a) Global vegetation model

First, we consider; what absolute values of resilience and trends in resilience should we expect across different biomes and ecosystems? There is remarkably little research on this. To begin to address it, we undertake an illustrative analysis of results from a dynamic global vegetation model with land-use (LPJmL) forced with output from a climate model (GFDL-ESM2M), obtained from the Inter-Sectoral Impact Model Inter-comparison Project (ISIMIP, round 2b) [74, 75]. We focus on the AR(1) of modelled NPP as an indicator of whole plant resilience, and the interval 2000-2019, so that we can then compare results to analysis of remotely sensed data. The climate input is bias corrected and follows the historical model run to 2005 and the RCP8.5 scenario thereafter, which most closely tracks actual emissions up to 2020 [76].

Mean AR(1) of monthly NPP (2000-2019), having removed the seasonal cycle and trend in each location, shows clear spatial structure (Figure 1a). AR(1) is highest (lowest resilience) in some dry regions and lowest (highest resilience) in some temperate ecosystems and e.g. on the wet edge of the Sahel. Negative AR(1) values, which occur across parts of the boreal regions and also e.g. in the eastern Himalayan plateau, suggest poor fit of an autoregressive model and should be ignored. Overall, there is some hint that wetter locations tend to have greater resilience of modelled NPP than drier locations.

The trend in AR(1) of monthly NPP (2000-2019) shows a variable spatial picture (Figure 1b), with no significant global average trend ($\tau$=-0.08). The spatial scatter suggests internal variability, including of the climate input, influences the trends. An overall anthropogenic forcing signal should bring some spatial coherence, even if manifesting through e.g. complex-structured changes in the hydrological cycle. There is some spatially coherent behaviour, including loss of resilience in e.g. southwest North America, Central America, the southeast Amazon, Caatinga, and Gran Chaco of South America. Some of these regions have been experiencing drought with an anthropogenic forcing component [77, 78]. However, internal (multi)decadal climate variability also influences drought and in one instance of a climate model, the timing of internal variability is unlikely to match reality.

Other recent work has analysed annual GPP from a large ensemble of climate models' future projections [79], using the ratio of the squared mean and variance of annual GPP as a 'resilience indicator', proportional to the return period of the largest tolerable perturbation. This assumes a multi-year timescale of recovery, when it can be sub-annual [53-55]. Notable is a predicted increase in inter-annual GPP variability across much of the tropics under high-end climate forcing, especially in the Amazon [79].

## (b) Global data

Turning to global analysis of remotely sensed data, a benchmark study [59] considered different measures of resilience of NDVI (2001-2006) including AR(1), spectral entropy, spectral scaling, and their reliability to different types of noise, comparing to in situ observations at 1085 locations. Resilience (1 – AR(1)) was found to be high in forests and lower in shrubland, (woody) savannah, and grasslands. Subsequent work [80] fitted an autoregressive model for NDVI (1981-2006) that converges in 77.5% of terrestrial pixels, with regions of poor fit in high northern latitudes, coastal, desert or

tropical regions. In the remaining regions, AR(1) is highest (lowest resilience) in semi-arid settings across the planet with low tree cover and high bare soil fraction. Lowest AR(1) (highest resilience) is seen in temperate ecosystems and on the wet edge of the Sahel, where there is high tree cover and low bare soil fraction. Some other published global studies use measures of 'resilience' that are not directly related to recovery rate [16, 21]: LAI maximum stress/recovery time also shows maxima in tropical forests and minima in semi-arid regions [21], whereas GPP drought recovery time is longest in some tropical rainforests [16].

Following [80], we have targeted NDVI at monthly resolution (here 2001-2020 from MODIS), utilising the Google Earth Engine (GEE) software portal and cloud compute capability as a platform, and introduced algorithms to calculate AR(1), having removed the mean seasonal cycle and trend in each location (Figure 2a). We filter out locations with NDVI<0.18, which removes ice sheets and deserts. Some boreal locations have AR(1)<0 and should be ignored. The mean AR(1) shows spatial patterns (Figure 2a) consistent with earlier work [80] (although we have not filtered for goodness of model fit). There is a positive correlation with AR(1) of modelled NPP (Figure 1a) – excluding pixels with negative AR(1) values; Pearson's $r$=0.44, Spearman's $\rho$=0.41 (both $p<10^{-6}$) – despite differences in spatial pattern and NDVI being only indirectly related to NPP. Resilience of NDVI is lowest in semi-arid regions and highest in tropical forests, indicating a clear dependence on precipitation.

Some existing studies have started to consider trends in 'resilience' over time, but do not present a mean value as a baseline, and use composite indicators that do not isolate recovery rate [56, 57]. Trends in a composite indicator of autocorrelation, standard deviation, skewness and kurtosis of NDVI over 1981-2015 hints at greatest loss of 'resilience' in the tundra [56]. A more confusing composite indicator hints at primary production showing greatest 'resilience' loss in tundra and boreal forest [57]. However, these are regions where our results and previous studies [80] suggest poor fit of an autoregressive model.

In an attempt to isolate changes in recovery rate, we consider trends in AR(1) of monthly NDVI (MODIS) over 2001-2020 (Figure 2b). These trends could be (partly) due to internal decadal climate variability [81] and we have not assessed their statistical significance. Nevertheless, in the global average, AR(1) has increased (resilience has declined); excluding rock/ice and desert biomes, and pixels with negative mean AR(1) values, $\tau$=0.61. Despite a scattered spatial picture, there are some spatially coherent regions of consistent trends. Pronounced increases in AR(1) (resilience loss) are seen in e.g. the Eastern Mediterranean, Central America, and the Caatinga (northeast Brazil), all of which have been experiencing prolonged drought, potentially with an anthropogenic forcing component [77]. Despite no overall correlation (Pearson's $r$=-0.024, Spearman's $\rho$=-0.025) with our model predicted changes in resilience of NPP (Figure 1b), in these regions, there is some agreement over resilience loss.

## (c) Biomes-ecoregions

Particular biomes or ecoregions that may be vulnerable to abrupt transitions or 'tipping points' [5] and are therefore priority targets for resilience sensing include: tropical forests and savannahs [35, 36, 71]; boreal forests, tundra and permafrost [82, 83]. Existing resilience studies (Table 1) span an eclectic mix of biomes including tropical forest, savannah, and Mediterranean ones. Sometimes they add spatial resolution to global studies (but rarely temporal resolution). Early work on Mediterranean forest, woodland and scrubland extracted variation in recovery rate across landscapes [54, 55]. Global analyses already indicate fundamental differences in resilience of NDVI across biomes (Figure 2a), and hint at differing trends in resilience across biomes (Figure 2b).

Aggregating the AR(1) trend results (Figure 2b) by biome (excluding deserts and xeric shrub lands) reveals that the strongest increasing trends of AR(1) of NDVI (2000-2020) are in tropical and subtropical dry broadleaf forests ($\tau$=0.72), montane grasslands and shrublands ($\tau$=0.69), and temperate coniferous forests ($\tau$=0.63) (although their significance has not been tested). Zooming into a region of South and East Asia that spans all three of these biomes, we can pick out example ecoregions with positive AR(1) trends (Figure 3): In India, the Central Deccan Plateau dry deciduous forests ($\tau$ =0.67). In western China, a group of conifer forest ecoregions, especially the Hengduan Mountains subalpine conifer forests ($\tau$ =0.78) and Qionglai-Minshan conifer forests ($\tau$ =0.79). Also, a large part of the Mongolian steppe appears to have a coherent loss of resilience, including part of the Ordos Plateau steppe montane grassland ($\tau$ =0.62).

Tropical forest biomes show mixed trends in AR(1) of NDVI (Figure 2b), but typically have a low mean AR(1) (Figure 2a). Instead, VOD can provide a better proxy for fluctuations in aboveground biomass [64]. Within tropical forests biomes, AR(1) of NDVI and VOD both show a general decrease in resilience as mean annual precipitation (MAP) drops below ~2000 mm $yr^{-1}$ [34]. Recent work, focused on the Amazon shows an overall pronounced increase in AR(1) of VOD (decline in resilience) since the early 2000s [64]. AR(1) of NDVI shows a less consistent signal (Figure 2b), but has also increased [64]. Observed increases in AR(1) of VOD (and NDVI) are generally greater in drier parts of the Amazon and closer to human settlements and roads [64]. This is consistent with inferences from multi-modality of tree cover [35, 36, 67] that in some locations tropical forest and savannah can represent alternative stable states under the same climate

boundary conditions – although confounding variables need to be carefully accounted for [67]. Resilience is predicted to decline along gradients of decreasing rainfall for woodland/forest, or increasing rainfall for grassland/savannah. This hypothesis has been tested on other continents using spatial resilience indicators and leveraging high spatial resolution remote sensing data. Peaks of spatial variance and spatial correlation were found to correspond to regions of inferred bi-modality of EVI along forest-savannah gradients in Australia and Congo-Gabon [40]. Increasing spatial variance, spatial correlation, spatial skewness, and spatial spectra are also found along spatial gradients from grassland to woodland in Serengeti-Mara (where bi-stability is not expected) [39, 40] – emphasising that resilience loss does not necessarily imply an approaching tipping point (Box 1).

## (d) Ecosystems

The highest spatial resolution satellite remote sensing can enable zooming into resilience at ~10 m ecosystem scales, including resolving highly spatially heterogeneous perturbations such as fires – although our prototype global portal (Figures 2 and 3) is not yet set up to zoom in to this resolution. Even higher resolution is achievable with airborne remote sensors e.g. [31]. Existing studies (Table 1) examine just a small subset of ecosystems, but they overlap with some particularly vulnerable ones including Mediterranean vegetation, savannas, and California woodland. Some ecosystems may be particularly vulnerable to abrupt change and/or tipping points due to localised feedbacks, including forests subject to dieback [84], peatlands [85], and regularly patterned vegetation [86] (although see [87] on the latter). Indeed, analysis of Californian forests at fine spatial and temporal resolution has revealed statistical early warning signals of rising AR(1) of NDVI prior to forest dieback mortality events [88], increasing confidence that resilience sensing can help highlight where tipping points may be prone to occurring.

Analysis of UK peatlands water table depth (measured with synthetic-aperture radar; SAR) at fine spatial and temporal resolution has revealed varying recovery time of water table depth from drought, picking up areas of greater drainage (both natural and anthropogenic) and of more severe erosion (gullying) as having longer recovery times (compared to nearby locations experiencing comparable perturbation) [17]. Varying recovery time from vegetation management – traditionally by fires – shows that larger and more severe management interventions (measured with difference Normalised Burn Ratio; dNBR) lead to longer recovery times of NDVI [18]. However, further work is needed to extract recovery rates from the large amounts of data.

Regular patterns of dryland vegetation are a manifestation of competing positive and negative feedbacks on fine spatial scales of order ~10-100 m, so require fine spatial resolution satellite remote sensing to be resolved. Spatial skewness may track vegetation patterning along environmental gradients but at questionably coarse spatial resolution (400 m) [89]. Instead feature vectors applied to 10 m resolution data allow the nature of patterning to be converted to a metric [42, 90], which can then be tracked temporally [42]. Treating seasonal rains as a perturbation, recovery time can be directly extracted and compared to AR(1) estimated after the seasonal cycle has been removed [42]. They give consistent resilience results, including across mean annual precipitation (MAP) gradients [42].

# 5. Discussion

## (a) Advancing resilience governance and management

Resilience sensing could inform several scales of biosphere governance and management and address a widely stated critical knowledge gap. Internationally, the Convention on Biological Diversity (CBD) includes, as part of Aichi biodiversity target 15, enhancing ecosystem resilience. However, the Intergovernmental Science-Policy Platform on Biodiversity and Ecosystem Services (IPBES) [91] reports that progress towards this target is "unknown" highlighting it as a knowledge gap and stating that: "the lack of both quantitative indicators and qualitative information means that no assessment of progress was possible". As we have reviewed, quantitative indicators and qualitative information are available, and a resilience sensing system could help provide a regular status report on biosphere resilience that could form part of IPBES assessment reports.

At the national level, a resilience sensing system could help provide regular national biosphere resilience assessments. This is particularly pertinent within the UK, which recently passed into law an Environment Act (2021) that requires 'local nature recovery strategies' for all areas of England. Already, The Well-being of Future Generations (Wales) Act (2015) has as one of its goals a resilient Wales including "healthy functioning ecosystems that support social, economic, and ecological resilience". Furthermore, The Environment (Wales) Act (2016) gives National Resources Wales (the national environment agency) under the Sustainable Management of Natural Resources (SMNR), the Aim 2: Ecosystems are Resilient to Expected and Unforeseen Change. These two Acts require that public bodies in Wales work to maintain or enhance ecosystem resilience but currently "a major impediment to this objective is the difficulty of practically

measuring resilience for management purposes" [92]. A pragmatic approach currently used focuses on attributes of diversity, extent, condition, connectivity, and adaptability ('DECCA') that have previously been causally linked with ecosystem resilience [92]. A resilience sensing system can offer a more direct (and complementary) approach.

At the regional-to-local level, a resilience sensing system could help governance authorities and land managers identify locations to target actions to increase resilience, and to monitor progress towards resilience goals. Particularly pertinent are conservation areas and their associated governance bodies, including national parks. National parks around the world are beginning to make increasing resilience a goal, often framed in terms of resilience to climate change – i.e. a wider factor not under their direct control. For example, in the UK, the Management Plan for Dartmoor National Park (2021) has as part of its vision to make Dartmoor "climate resilient". Dartmoor's blanket peat biome is particularly vulnerable to climate change [93], and existing resilience sensing results already suggest where recovery rate of the water table from drought events is slowest [17].

Other studies are starting to monitor resilience within managed lands of sub-Saharan Africa (Table 1). This raises the critical question of how resilience sensing can become useful for land managers on the ground. A computational cloud-based resilience sensing system/portal could empower local users seeking to enhance ecological resilience and facilitate international knowledge exchange. This is particularly important for those without access to local high performance computing power. For example, in the semi-arid rangelands of Africa, land-users and managers are increasingly seeking to adapt management practices to reverse long-term trends of degradation and enhance resilience of ecosystem service provision, and thus livelihoods. In many cases, they are already using remote sensing products to monitor ecosystem health and productivity, distribution of invasive species, or other key indicators to facilitate adaptive management [94]. To maximise its potential, a global portal needs to be interactive, allowing the user to define areas of interest and repeat automated analyses over time, to assess whether management interventions are having an effect.

## (b) Limitations and further research

Our synthesis of review and research serves to illustrate the potential (and some pitfalls) of a resilience sensing system for the terrestrial biosphere. A practical limitation in applying resilience sensing is the potential mismatch of timescales between getting feedback from resilience sensing and altering actions affecting resilience. Vegetation resilience has timescales of order a month to a few years, although detecting statistically significant changes in resilience takes longer. The timescale of enacting governance and management changes depends on the spatial scale. Local management interventions could conceivably change resilience relatively rapidly, whereas governance of global change appears woefully slow, and the change itself – especially climate change – contains considerable inertia.

Methodological and application limitations invite many avenues for further research and development. Among the most important: The most appropriate remote sensing products and method of resilience sensing depends on the ecological and management context (i.e. the resilience of what to what that a scientist or manager seeks to monitor) and needs to be deduced. Different remote sensing proxies appear better for different biomes-ecoregions-ecosystems, even when the focus is just on vegetation resilience. Resilience in NDVI patterns is not always equivalent to resilience in the provision of ecosystem services. When looking beyond vegetation to resilience of ecosystem properties (e.g. tree fraction, water table depth) other proxies need to be assessed. Crucial to that assessment are; consideration of how noise in remote sensing proxies affects resilience indicators, assessing model adequacy, and testing purported signals against null models – i.e. increasing the rigour of analyses.

Fundamental work is needed to assess what can give rise to observed trends in e.g., AR(1) (Figures 2b, 3). Further dynamic global vegetation model experiments (e.g. Figure 1b), subject to observed climate variability, different climate forcing and land-use change scenarios, can help assess what trends in resilience to expect across different biomes and ecosystems under different types of forcing. The effect of ongoing land-use changes on resilience can be examined in remotely sensed data, e.g. comparing resilience trends in neighbouring locations with differing land-use change. Statistical research is warranted to assess how long a sampling interval is required to pick up significant trends in resilience. Automating the assessment of model fit and significance testing against null models could form a valuable 'screening' part of a portal. To address how spatial scale affects resilience expectations, both fine-resolution model output and data can be aggregated to coarser spatial scales to assess how this affects resilience indicators. Exploiting the high spatial resolution of remotely sensed data by expanding and exploring the application of spatial resilience indicators offers a key opportunity. Theoretical work could e.g. aggregate the results of an existing spatial model [95] to larger 'pixel' sizes to assess the robustness of spatial autocorrelation as a resilience indicator.

Looking more broadly: There is the potential to bring other data streams into a resilience sensing system. For the terrestrial biosphere, this could start with e.g. existing data from the FLUXNET global network of micrometeorological sites, and the US long-term ecological research (LTER) network of sites. At one LTER site, a resilience indicator has already been shown to usefully forewarn of a grassland to shrubland state transition [96]. Remote sensing of biosphere

resilience could be extended to marine and freshwater aquatic ecosystems, including lakes [48], where experimental studies show that resilience indicators work [97]. Satellite remote sensing is restricted to shallow water depths, but autonomous vehicle sampling can help address this. A further key opportunity is to extend resilience sensing to social-ecological systems by integrating social and ecological data, including through social sensing [98] and citizen science initiatives [99].

## 6. Conclusion

We have outlined how a biosphere resilience sensing system could raise collective awareness of risks to our life-support systems, making it easier to see where ecosystem resilience is declining, and to see whether deliberate efforts to increase resilience are working. We have anchored on a simple but mathematically rigorous definition of resilience as recovery rate from perturbations. Others will no doubt highlight other aspects of 'resilience' that should be considered. We simply ask that these are clearly defined and quantifiable, with definitions consistently applied – then they can be added to a resilience sensing system. We also chose to focus on the terrestrial biosphere, satellite remote sensing, and advances in software and cloud computing. However, we recognise that the aquatic and marine biosphere is just as important, that direct observations are often more accurate, and that the greatest value of technology may be to increase usability and accessibility. Our critical review of existing efforts to remotely sense the resilience of the terrestrial biosphere suggests a very mixed bag – ranging from outright failure to rigorous consideration of statistical robustness. There has been remarkably little consideration of what subset of biosphere resilience remote sensing allows us to monitor. Nevertheless, existing work and our illustrative results do show how resilience sensing can be nested across scales, could aid management and governance at these different scales, and can address a widely stated critical gap in quantitative indicators of resilience. There is clearly much room for further research and development, but the task could not be more salient or timely. If we can better sense where resilience is being lost then we have a better chance of correcting our mistakes, and if we can better sense where things are going right then we can learn something about which positive actions we should seek to replicate.

## Acknowledgments

TML, JEB, DIAM, CAB, KL were supported by the Leverhulme Trust (RPG-2018-046). TML was supported by the Alan Turing Institute (Turing Fellowship). DIAM was supported by the European Research Council (Earth Resilience in the Anthropocene project, grant no. ERA 743080). NB acknowledges funding by the Volkswagen foundation and the European Union's Horizon 2020 research and innovation programme under grant agreement No. 820970 (TiPES). We thank Jim Lovelock and Bruno Latour for inspiration, and the ISIMIP team for model output.

# References

[1] Lenton, T. M. & Latour, B. 2018 Gaia 2.0. *Science* **361**, 1066-1068.
[2] Holling, C. S. 1973 Resilience and stability of ecological systems. *Annual Review of Ecology and Systematics* **4**, 1-23.
[3] Lovelock, J. E. 1972 Gaia as seen through the atmosphere. *Atmospheric Environment* **6**, 579-580.
[4] Scheffer, M., Carpenter, S., Foley, J. A., Folke, C. & Walker, B. 2001 Catastrophic shifts in ecosystems. *Nature* **413**, 591-596. (DOI:10.1038/35098000).
[5] Lenton, T. M., Held, H., Kriegler, E., Hall, J., Lucht, W., Rahmstorf, S. & Schellnhuber, H. J. 2008 Tipping Elements in the Earth's Climate System. *Proceedings of the National Academy of Sciences* **105**, 1786-1793. (DOI:10.1073/pnas.0705414105).
[6] Carpenter, S., Walker, B., Anderies, J. M. & Abel, N. 2001 From Metaphor to Measurement: Resilience of What to What? *Ecosystems* **4**, 765-781. (DOI:10.1007/s10021-001-0045-9).
[7] Pimm, S. L. 1984 The complexity and stability of ecosystems. *Nature* **307**, 321-326.
[8] Grimm, V. & Wissel, C. 1997 Babel, or the ecological stability discussions: an inventory and analysis of terminology and a guide for avoiding confusion. *Oecologia* **109**, 323-334. (DOI:10.1007/s004420050090).
[9] Kéfi, S., Domínguez-García, V., Donohue, I., Fontaine, C., Thébault, E. & Dakos, V. 2019 Advancing our understanding of ecological stability. *Ecology Letters* **22**, 1349-1356. (DOI:10.1111/ele.13340).
[10] Walker, B. H. 2020 Resilience: what it is and is not. *Ecology and Society* **25**. (DOI:10.5751/ES-11647-250211).
[11] Cañizares, J. C., Copeland, S. M. & Doorn, N. 2021 Making Sense of Resilience. *Sustainability* **13**, 8538.
[12] Lenton, T. M., Daines, S. J., Dyke, J. G., Nicholson, A. E., Wilkinson, D. M. & Williams, H. T. P. 2018 Selection for Gaia across multiple scales. *Trends in Ecology & Evolution* **33**, 633-645. (DOI:10.1016/j.tree.2018.05.006).

[13] Holling, C. S. 1996 Engineering Resilience versus Ecological Resilience. In *Engineering within Ecological Constraints* (ed. P. E. Schulze), pp. 31-43. Washington DC, National Academy Press.
[14] Wissel, C. 1984 A universal law of the characteristic return time near thresholds. *Oecologia* **65**, 101-107. (DOI:10.1007/bf00384470).
[15] van Nes, E. H. & Scheffer, M. 2007 Slow Recovery from Perturbations as a Generic Indicator of a Nearby Catastrophic Shift. *American Naturalist* **169**, 738-747.
[16] Schwalm, C. R., Anderegg, W. R. L., Michalak, A. M., Fisher, J. B., Biondi, F., Koch, G., Litvak, M., Ogle, K., Shaw, J. D., Wolf, A., et al. 2017 Global patterns of drought recovery. *Nature* **548**, 202. (DOI:10.1038/nature23021).
[17] Lees, K. J., Artz, R. R. E., Chandler, D., Aspinall, T., Boulton, C. A., Buxton, J., Cowie, N. R. & Lenton, T. M. 2021 Using remote sensing to assess peatland resilience by estimating soil surface moisture and drought recovery. *Science of The Total Environment* **761**, 143312. (DOI:10.1016/j.scitotenv.2020.143312).
[18] Lees, K. J., Buxton, J., Boulton, C. A., Abrams, J. F. & Lenton, T. M. 2021 Using satellite data to assess management frequency and rate of regeneration on heather moorlands in England as a resilience indicator. *Environmental Research Communications* **3**, 085003. (DOI:10.1088/2515-7620/ac1a5f).
[19] Mageau, M. T., Costanza, R. & Ulanowicz, R. 1995 The development and initial testing a quantitative assessment of ecosystem health. *Ecosystem Health* **1**, 201-213.
[20] White, H. J., Gaul, W., Sadykova, D., León-Sánchez, L., Caplat, P., Emmerson, M. C. & Yearsley, J. M. 2020 Quantifying large-scale ecosystem stability with remote sensing data. *Remote Sensing in Ecology and Conservation* **6**, 354-365. (DOI:10.1002/rse2.148).
[21] Wu, J. & Liang, S. 2020 Assessing Terrestrial Ecosystem Resilience using Satellite Leaf Area Index. *Remote Sensing* **12**, 595.
[22] Carpenter, S. R. & Brock, W. A. 2006 Rising variance: a leading indicator of ecological transition. *Ecology Letters* **9**, 311-318. (DOI:10.1111/j.1461-0248.2005.00877.x).
[23] Lenton, T. M. 2011 Early warning of climate tipping points. *Nature Climate Change* **1**, 201-209. (DOI:10.1038/nclimate1143).
[24] Scheffer, M., Bacompte, J., Brock, W. A., Brovkin, V., Carpenter, S. R., Dakos, V., Held, H., van Nes, E. H., Rietkerk, M. & Sugihara, G. 2009 Early warning signals for critical transitions. *Nature* **461**, 53-59.
[25] Scheffer, M., Carpenter, S. R., Lenton, T. M., Bascompte, J., Brock, W., Dakos, V., van de Koppel, J., van de Leemput, I. A., Levin, S. A., van Nes, E. H., et al. 2012 Anticipating Critical Transitions. *Science* **338**, 344-348. (DOI:10.1126/science.1225244).
[26] Box, G. E. P. & Tiao, G. C. 1975 Intervention Analysis with Applications to Economic and Environmental Problems. *Journal of the American Statistical Association* **70**, 70-79. (DOI:10.2307/2285379).
[27] Dakos, V., van Nes, E. H., D'Odorico, P. & Scheffer, M. 2012 Robustness of variance and autocorrelation as indicators of critical slowing down. *Ecology* **93**, 264-271. (DOI:10.1890/11-0889.1).
[28] Kuehn, C. 2011 A mathematical framework for critical transitions: bifurcations, fast-slow systems and stochastic dynamics. *Physica D: Nonlinear Phenomena* **2010**, 1-20.
[29] Bury, T. M., Sujith, R. I., Pavithran, I., Scheffer, M., Lenton, T. M., Anand, M. & Bauch, C. T. 2021 Deep learning for early warning signals of regime shifts. *Proceedings of the National Academy of Sciences*, in press. (DOI:10.1101/2021.03.28.437429).
[30] Dakos, V., Carpenter, S. R., Brock, W. A., Ellison, A. M., Guttal, V., Ives, A. R., Kefi, S., Livina, V., Seekell, D. A., van Nes, E. H., et al. 2012 Methods for Detecting Early Warnings of Critical Transitions in Time Series Illustrated Using Simulated Ecological Data. *PLoS ONE* **7**, e41010.
[31] van Belzen, J., van de Koppel, J., Kirwan, M. L., van der Wal, D., Herman, P. M. J., Dakos, V., Kéfi, S., Scheffer, M., Guntenspergen, G. R. & Bouma, T. J. 2017 Vegetation recovery in tidal marshes reveals critical slowing down under increased inundation. *Nature Communications* **8**, 15811. (DOI:10.1038/ncomms15811).
[32] van Belzen, J., van de Koppel, J., van der Wal, D., Herman, P. M. J., Dakos, V., Kéfi, S., Scheffer, M. & Bouma, T. J. 2017 Timing recovery of ecosystems in sequential remotely sensed and simulated data.
[33] Cole, L. E. S., Bhagwat, S. A. & Willis, K. J. 2014 Recovery and resilience of tropical forests after disturbance. *Nature Communications* **5**, 3906. (DOI:10.1038/ncomms4906).
[34] Verbesselt, J., Umlauf, N., Hirota, M., Holmgren, M., Van Nes, E. H., Herold, M., Zeileis, A. & Scheffer, M. 2016 Remotely sensed resilience of tropical forests. *Nature Clim. Change* **6**, 1028-1031. (DOI:10.1038/nclimate3108).
[35] Hirota, M., Holmgren, M., Van Nes, E. H. & Scheffer, M. 2011 Global Resilience of Tropical Forest and Savanna to Critical Transitions. *Science* **334**, 232-235. (DOI:10.1126/science.1210657).
[36] Staver, A. C., Archibald, S. & Levin, S. A. 2011 The Global Extent and Determinants of Savanna and Forest as Alternative Biome States. *Science* **334**, 230-232. (DOI:10.1126/science.1210465).
[37] Dakos, V., van Nes, E., Donangelo, R., Fort, H. & Scheffer, M. 2010 Spatial correlation as leading indicator of catastrophic shifts. *Theoretical Ecology* **3**, 163-174. (DOI:10.1007/s12080-009-0060-6).
[38] Kéfi, S., Guttal, V., Brock, W. A., Carpenter, S. R., Ellison, A. M., Livina, V. N., Seekell, D. A., Scheffer, M., van Nes, E. H. & Dakos, V. 2014 Early Warning Signals of Ecological Transitions: Methods for Spatial Patterns. *PLOS ONE* **9**, e92097. (DOI:10.1371/journal.pone.0092097).

[39] Eby, S., Agrawal, A., Majumder, S., Dobson, A. P. & Guttal, V. 2017 Alternative stable states and spatial indicators of critical slowing down along a spatial gradient in a savanna ecosystem. *Global Ecology and Biogeography* **26**, 638-649. (DOI:10.1111/geb.12570).
[40] Majumder, S., Tamma, K., Ramaswamy, S. & Guttal, V. 2019 Inferring critical thresholds of ecosystem transitions from spatial data. *Ecology* **100**, e02722. (DOI:10.1002/ecy.2722).
[41] Tirabassi, G. & Masoller, C. 2022 Correlation lags give early warning signals of approaching bifurcations. *Chaos, Solitons & Fractals* **155**, 111720. (DOI:10.1016/j.chaos.2021.111720).
[42] Buxton, J. E., Abrams, J. F., Boulton, C. A., Barlow, N., Rangel Smith, C., Van Stroud, S., Lees, K. J. & Lenton, T. M. 2021 Quantitatively Monitoring the Resilience of Patterned Vegetation in the Sahel. *Global Change Biology* **28**, 571-587. (DOI:10.1111/gcb.15939).
[43] Yin, Z., Dekker, S. C., Rietkerk, M., van den Hurk, B. J. J. M. & Dijkstra, H. A. 2016 Network based early warning indicators of vegetation changes in a land–atmosphere model. *Ecological Complexity* **26**, 68-78. (DOI:10.1016/j.ecocom.2016.02.004).
[44] Tirabassi, G., Viebahn, J., Dakos, V., Dijkstra, H. A., Masoller, C., Rietkerk, M. & Dekker, S. C. 2014 Interaction network based early-warning indicators of vegetation transitions. *Ecological Complexity* **19**, 148-157. (DOI:10.1016/j.ecocom.2014.06.004).
[45] Boulton, C. A. & Lenton, T. M. 2015 Slowing down of North Pacific climate variability and its implications for abrupt ecosystem change. *PNAS* **112**, 11496-11501. (DOI:10.1073/pnas.1501781112).
[46] Dakos, V., Scheffer, M., van Nes, E. H., Brovkin, V., Petoukhov, V. & Held, H. 2008 Slowing down as an early warning signal for abrupt climate change. *PNAS* **105**, 14308-14312.
[47] Rypdal, M. 2016 Early-Warning Signals for the Onsets of Greenland Interstadials and the Younger Dryas–Preboreal Transition. *Journal of Climate* **29**, 4047-4056. (DOI:10.1175/jcli-d-15-0828.1).
[48] Alibakhshi, S., Groen, T., Rautiainen, M. & Naimi, B. 2017 Remotely-Sensed Early Warning Signals of a Critical Transition in a Wetland Ecosystem. *Remote Sensing* **9**, 352.
[49] Lanfredi, M., Simoniello, T. & Macchiato, M. 2004 Temporal persistence in vegetation cover changes observed from satellite: Development of an estimation procedure in the test site of the Mediterranean Italy. *Remote Sensing of Environment* **93**, 565-576. (DOI:10.1016/j.rse.2004.08.012).
[50] Simoniello, T., Lanfredi, M., Liberti, M., Coppola, R. & Macchiato, M. 2008 Estimation of vegetation cover resilience from satellite time series. *Hydrol. Earth Syst. Sci.* **12**, 1053-1064. (DOI:10.5194/hess-12-1053-2008).
[51] Cui, X., Gibbes, C., Southworth, J. & Waylen, P. 2013 Using Remote Sensing to Quantify Vegetation Change and Ecological Resilience in a Semi-Arid System. *Land* **2**, 108-130.
[52] Harris, A., Carr, A. S. & Dash, J. 2014 Remote sensing of vegetation cover dynamics and resilience across southern Africa. *International Journal of Applied Earth Observation and Geoinformation* **28**, 131-139. (DOI:10.1016/j.jag.2013.11.014).
[53] Telesca, L. & Lasaponara, R. 2006 Pre- and post-fire behavioral trends revealed in satellite NDVI time series. *Geophysical Research Letters* **33**. (DOI:10.1029/2006GL026630).
[54] Telesca, L. & Lasaponara, R. 2006 Quantifying intra-annual persistent behaviour in SPOT-VEGETATION NDVI data for Mediterranean ecosystems of southern Italy. *Remote Sensing of Environment* **101**, 95-103. (DOI:10.1016/j.rse.2005.12.007).
[55] Telesca, L., Lasaponara, R. & Lanorte, A. 2008 Intra-annual dynamical persistent mechanisms in mediterranean ecosystems revealed SPOT-VEGETATION time series. *Ecological Complexity* **5**, 151-156. (DOI:10.1016/j.ecocom.2007.10.001).
[56] Feng, Y., Su, H., Tang, Z., Wang, S., Zhao, X., Zhang, H., Ji, C., Zhu, J., Xie, P. & Fang, J. 2021 Reduced resilience of terrestrial ecosystems locally is not reflected on a global scale. *Communications Earth & Environment* **2**, 88. (DOI:10.1038/s43247-021-00163-1).
[57] Rocha, J. C. 2022 Ecosystems are showing symptoms of resilience loss. (arXiv:2107.03307).
[58] Myers-Smith, I. H., Kerby, J. T., Phoenix, G. K., Bjerke, J. W., Epstein, H. E., Assmann, J. J., John, C., Andreu-Hayles, L., Angers-Blondin, S., Beck, P. S. A., et al. 2020 Complexity revealed in the greening of the Arctic. *Nature Climate Change* **10**, 106-117. (DOI:10.1038/s41558-019-0688-1).
[59] De Keersmaecker, W., Lhermitte, S., Honnay, O., Farifteh, J., Somers, B. & Coppin, P. 2014 How to measure ecosystem stability? An evaluation of the reliability of stability metrics based on remote sensing time series across the major global ecosystems. *Global Change Biology* **20**, 2149-2161. (DOI:10.1111/gcb.12495).
[60] Zhang, L., Zhou, D., Fan, J., Guo, Q., Chen, S., Wang, R. & Li, Y. 2019 Contrasting the Performance of Eight Satellite-Based GPP Models in Water-Limited and Temperature-Limited Grassland Ecosystems. *Remote Sensing* **11**, 1333.
[61] Liang, S., Zhao, X., Liu, S., Yuan, W., Cheng, X., Xiao, Z., Zhang, X., Liu, Q., Cheng, J., Tang, H., et al. 2013 A long-term Global LAnd Surface Satellite (GLASS) data-set for environmental studies. *International Journal of Digital Earth* **6**, 5-33. (DOI:10.1080/17538947.2013.805262).
[62] Zhang, Q., Ge, L., Zhang, R., Metternicht, G. I., Du, Z., Kuang, J. & Xu, M. 2021 Deep-learning-based burned area mapping using the synergy of Sentinel-1&2 data. *Remote Sensing of Environment* **264**, 112575. (DOI:10.1016/j.rse.2021.112575).

[63] Bernardino, P. N., Brandt, M., De Keersmaecker, W., Horion, S., Fensholt, R., Storms, I., Wigneron, J.-P., Verbesselt, J. & Somers, B. 2020 Uncovering Dryland Woody Dynamics Using Optical, Microwave, and Field Data—Prolonged Above-Average Rainfall Paradoxically Contributes to Woody Plant Die-Off in the Western Sahel. *Remote Sensing* **12**, 2332.
[64] Boulton, C. A., Lenton, T. M. & Boers, N. in press Pronounced loss of Amazon rainforest resilience since the early 2000s. *Nature Climate Change*.
[65] Lenton, T. M., Kohler, T. A., Marquet, P. A., Boyle, R. A., Crucifix, M., Wilkinson, D. M. & Scheffer, M. 2021 Survival of the Systems. *Trends in Ecology & Evolution* **36**, 333-344. (DOI:10.1016/j.tree.2020.12.003).
[66] Scheffer, M., Hirota, M., Holmgren, M., Van Nes, E. H. & Chapin, F. S. 2012 Thresholds for boreal biome transitions. *Proceedings of the National Academy of Sciences* **109**, 21384-21389. (DOI:10.1073/pnas.1219844110).
[67] Wuyts, B., Champneys, A. R. & House, J. I. 2017 Amazonian forest-savanna bistability and human impact. *Nature Communications* **8**, 15519. (DOI:10.1038/ncomms15519).
[68] Abis, B. & Brovkin, V. 2017 Environmental conditions for alternative tree-cover states in high latitudes. *Biogeosciences* **14**, 511-527. (DOI:10.5194/bg-14-511-2017).
[69] Staal, A., Fetzer, I., Wang-Erlandsson, L., Bosmans, J. H. C., Dekker, S. C., van Nes, E. H., Rockström, J. & Tuinenburg, O. A. 2020 Hysteresis of tropical forests in the 21st century. *Nature Communications* **11**, 4978. (DOI:10.1038/s41467-020-18728-7).
[70] Bonan, G. B. 2008 Forests and Climate Change: Forcings, Feedbacks, and the Climate Benefits of Forests. *Science* **320**, 1444-1449.
[71] Boulton, C. A., Good, P. & Lenton, T. M. 2013 Early warning signals of simulated Amazon rainforest dieback. *Theoretical Ecology* **6**, 373-384. (DOI:10.1007/s12080-013-0191-7).
[72] Friedlingstein, P., Jones, M. W., O'Sullivan, M., Andrew, R. M., Bakker, D. C. E., Hauck, J., Le Quéré, C., Peters, G. P., Peters, W., Pongratz, J., et al. 2021 Global Carbon Budget 2021. *Earth Syst. Sci. Data Discuss.* **2021**, 1-191. (DOI:10.5194/essd-2021-386).
[73] Lovelock, J. E. 1991 *Gaia - The Practical Science of Planetary Medicine*. London, Gaia Books.
[74] Frieler, K., Lange, S., Piontek, F., Reyer, C. P. O., Schewe, J., Warszawski, L., Zhao, F., Chini, L., Denvil, S., Emanuel, K., et al. 2017 Assessing the impacts of 1.5 °C global warming – simulation protocol of the Inter-Sectoral Impact Model Intercomparison Project (ISIMIP2b). *Geosci. Model Dev.* **10**, 4321-4345. (DOI:10.5194/gmd-10-4321-2017).
[75] Reyer, C., Chang, J., Chen, M., Forrest, M., François, L., Henrot, A.-J., Hickler, T., Ito, A., Nishina, K., Ostberg, S., et al. 2019 ISIMIP2b Simulation Data from Biomes Sector. (GFZ Data Services. DOI:10.5880/PIK.2019.012.
[76] Schwalm, C. R., Glendon, S. & Duffy, P. B. 2020 RCP8.5 tracks cumulative CO2 emissions. *Proceedings of the National Academy of Sciences* **117**, 19656-19657. (DOI:10.1073/pnas.2007117117).
[77] Chiang, F., Mazdiyasni, O. & AghaKouchak, A. 2021 Evidence of anthropogenic impacts on global drought frequency, duration, and intensity. *Nature Communications* **12**, 2754. (DOI:10.1038/s41467-021-22314-w).
[78] Williams, A. P., Cook, E. R., Smerdon, J. E., Cook, B. I., Abatzoglou, J. T., Bolles, K., Baek, S. H., Badger, A. M. & Livneh, B. 2020 Large contribution from anthropogenic warming to an emerging North American megadrought. *Science* **368**, 314-318. (DOI:doi:10.1126/science.aaz9600).
[79] Zampieri, M., Grizzetti, B., Toreti, A., de Palma, P. & Collalti, A. 2021 Rise and fall of vegetation annual primary production resilience to climate variability projected by a large ensemble of Earth System Models' simulations. *Environmental Research Letters* **16**, 105001. (DOI:10.1088/1748-9326/ac2407).
[80] De Keersmaecker, W., Lhermitte, S., Tits, L., Honnay, O., Somers, B. & Coppin, P. 2015 A model quantifying global vegetation resistance and resilience to short-term climate anomalies and their relationship with vegetation cover. *Global Ecology and Biogeography* **24**, 539-548. (DOI:10.1111/geb.12279).
[81] Lenton, T. M., Dakos, V., Bathiany, S. & Scheffer, M. 2017 Observed trends in the magnitude and persistence of monthly temperature variability. *Scientific Reports* **7**, 5940. (DOI:10.1038/s41598-017-06382-x).
[82] Lucht, W., Schaphoff, S., Erbrecht, T., Heyder, U. & Cramer, W. 2006 Terrestrial vegetation redistribution and carbon balance under climate change. *Carbon Balance and Management* **1**, 6. (DOI:doi:10.1186/1750-0680-1-6).
[83] Vaks, A., Gutareva, O. S., Breitenbach, S. F. M., Avirmed, E., Mason, A. J., Thomas, A. L., Osinzev, A. V., Kononov, A. M. & Henderson, G. M. 2013 Speleothems Reveal 500,000-Year History of Siberian Permafrost. *Science* **340**, 183-186. (DOI:10.1126/science.1228729).
[84] Allen, C. D., Macalady, A. K., Chenchouni, H., Bachelet, D., McDowell, N., Vennetier, M., Kitzberger, T., Rigling, A., Breshears, D. D., Hogg, E. H., et al. 2010 A global overview of drought and heat-induced tree mortality reveals emerging climate change risks for forests. *Forest Ecology and Management* **259**, 660-684. (DOI:10.1016/j.foreco.2009.09.001).
[85] van der Velde, Y., Temme, A. J. A. M., Nijp, J. J., Braakhekke, M. C., van Voorn, G. A. K., Dekker, S. C., Dolman, A. J., Wallinga, J., Devito, K. J., Kettridge, N., et al. 2021 Emerging forest–peatland bistability and resilience of European peatland carbon stores. *Proceedings of the National Academy of Sciences* **118**, e2101742118. (DOI:10.1073/pnas.2101742118).
[86] Rietkerk, M., Dekker, S. C., de Ruiter, P. C. & van de Koppel, J. 2004 Self-organized patchiness and catastrophic shifts in ecosystems. *Science* **305**, 1926-1929.

[87] Rietkerk, M., Bastiaansen, R., Banerjee, S., Koppel, J. v. d., Baudena, M. & Doelman, A. 2021 Evasion of tipping in complex systems through spatial pattern formation. *Science* **374**, eabj0359. (DOI:doi:10.1126/science.abj0359).
[88] Liu, Y., Kumar, M., Katul, G. G. & Porporato, A. 2019 Reduced resilience as an early warning signal of forest mortality. *Nature Climate Change* **9**, 880-885. (DOI:10.1038/s41558-019-0583-9).
[89] Veldhuis, M. P., Martinez-Garcia, R., Deblauwe, V. & Dakos, V. 2021 Remotely-sensed slowing down in spatially patterned dryland ecosystems. *bioRxiv*, 2021.2009.2027.461660. (DOI:10.1101/2021.09.27.461660).
[90] Mander, L., Dekker, S. C., Li, M., Mio, W., Punyasena, S. W. & Lenton, T. M. 2017 A morphometric analysis of vegetation patterns in dryland ecosystems. *Royal Society Open Science* **4**. (DOI:10.1098/rsos.160443).
[91] IPBES. 2019 *Global assessment report on biodiversity and ecosystem services of the Intergovernmental Science-Policy Platform on Biodiversity and Ecosystem Services*. IPBES secretariat, Bonn, Germany.
[92] Sanderson Bellamy, A., Latham, J., Spode, S., Ayling, S., Thomas, R. & Lindenbaum, K. 2021 A framework for ecosystem resilience in policy and practice: DECCA. *Ecology and Society* **26**. (DOI:10.5751/ES-12865-260431).
[93] Gallego-Sala, A. V. & Prentice, I. C. 2013 Blanket peat biome endangered by climate change. *Nature Clim. Change* **3**, 152-155. (DOI:10.1038/nclimate1672).
[94] Rangoonwala, A. & Ramsey, E. W., III. 2019 Monitoring live vegetation in semiarid and arid rangeland environments with satellite remote sensing in northern Kenya. (p. 83, U.S. Geological Survey.
[95] Kefi, S., Rietkerk, M., Alados, C. L., Pueyo, Y., Papanastasis, V. P., ElAich, A. & de Ruiter, P. C. 2007 Spatial vegetation patterns and imminent desertification in Mediterranean arid ecosystems. *Nature* **449**, 213-217.
[96] Ratajczak, Z., D'Odorico, P., Nippert, J. B., Collins, S. L., Brunsell, N. A. & Ravi, S. 2017 Changes in spatial variance during a grassland to shrubland state transition. *Journal of Ecology* **105**, 750-760. (DOI:10.1111/1365-2745.12696).
[97] Carpenter, S. R., Cole, J. J., Pace, M. L., Batt, R., Brock, W. A., Cline, T., Coloso, J., Hodgson, J. R., Kitchell, J. F., Seekell, D. A., et al. 2011 Early Warnings of Regime Shifts: A Whole-Ecosystem Experiment. *Science* **332**, 1079-1082. (DOI:10.1126/science.1203672).
[98] Liu, Y., Liu, X., Gao, S., Gong, L., Kang, C., Zhi, Y., Chi, G. & Shi, L. 2015 Social Sensing: A New Approach to Understanding Our Socioeconomic Environments. *Annals of the Association of American Geographers* **105**, 512-530. (DOI:10.1080/00045608.2015.1018773).
[99] Crain, R., Cooper, C. & Dickinson, J. L. 2014 Citizen Science: A Tool for Integrating Studies of Human and Natural Systems. *Annual Review of Environment and Resources* **39**, 641-665. (DOI:10.1146/annurev-environ-030713-154609).
[100] Verbesselt, J., Hyndman, R., Newnham, G. & Culvenor, D. 2010 Detecting trend and seasonal changes in satellite image time series. *Remote Sensing of Environment* **114**, 106-115. (DOI:10.1016/j.rse.2009.08.014).
[101] Verbesselt, J., Hyndman, R., Zeileis, A. & Culvenor, D. 2010 Phenological change detection while accounting for abrupt and gradual trends in satellite image time series. *Remote Sensing of Environment* **114**, 2970-2980. (DOI:10.1016/j.rse.2010.08.003).
[102] Verbesselt, J., Zeileis, A. & Herold, M. 2012 Near real-time disturbance detection using satellite image time series. *Remote Sensing of Environment* **123**, 98-108. (DOI:10.1016/j.rse.2012.02.022).

# Tables

**Table 1.** Remote sensing studies attempting to extract temporal or spatial indicators of terrestrial ecosystem resilience.

| **Scale, location** | **Year** | **Ref.** | **Vegetation, *perturbation*** | **Index(es)** (satellite/ database) | **Time-span** | **Resolution** (native) | | **'Resilience' metric(s)** | **Recovery rate?** |
|---|---|---|---|---|---|---|---|---|---|
| | | | | | | **Space*** | **Time** | | |
| **Global** | | | | | | | | | |
| World | 2014 | [59] | 15 land cover types | NDVI (MODIS) | 2001-2006 | 7 km (250 m) | 16 d | AR(1) , SD, CV, spectral entropy, spectral scaling | Yes (AR(1)) |
| World | 2015 | [80] | AR model fit subset | NDVI (GIMMS) | 1981-2006 | 0.072° | 1 mth (15 d) | AR(1) | Yes |
| World | 2017 | [16] | *drought* | GPP (MODIS) | 2000-2010 | 0.5° (1 km) | 1 mth (1 d) | recovery time | Not really |
| World | 2020 | [21] | *drought, fire* | LAI (GLASS, GIMMS) | 1982-2016 1982-2011 | 0.05° 0.083° | 8 d 15 d | max. stress /recovery time | Problematic |
| World | 2021 | [56] | | NDVI 3 g (GIMMS) | 1981-2015 | 0.083° | 1 mth | ACF-1, variance, skewness, kurtosis | Problematic (composite indicator) |
| World | pre-print | [57] | | GPP, ecosystem respiration (ESDL) | 2001-2018 | 0.25° | 7 d | AR(1), variance, skewness, kurtosis | No (speeding up included, composite indicator) |
| **Biome** | | | | | | | | | |
| S Italy | 2004 | [49] | forests, woods and scrub | NDVI (AVHRR) | 1985-1995 | 1.1 km | 1 y (1 d) | trend persistence | No |
| S Italy | 2006 | [54] | forests, woods and scrub | NDVI (SPOT-VEG.) | 1998-2003 | 1 km | 10 d | power spectral density, DFA | Yes |
| Sardinia | 2008 | [55] | shrub land, transitional, forest | NDVI, NDII (SPOT-VEG.) | 1998-2003 | 1 km | 10 d | DFA | Yes |
| Italy | 2008 | [50] | forests, woods and scrub | NDVI (GIMMS) | 1982-2003 | 8 km | 15 d | trend persistence | No |
| Kavango-Zambezi | 2013 | [51] | savannah | NDVI (TM/MSS Landsat) | 1973-2009 | 30-60 m | 22 images | trend persistence | No |
| Southern Africa | 2014 | [52] | 5 biomes | NDVI (GIMMS) | 1982-2006 | 5 km | 1 y (16 d) | trend persistence | No |
| Tropics | 2016 | [34] | tropical forests | NDVI (MODIS), VOD (AMSR-E) | 2000-2011 2002-2011 | 5.6 km 0.25° | 1 mth (8 d) 1 mth | AR(1) | Yes |
| Serengeti-Mara | 2017 | [39] | savannah | Woodland /grassland (ETM+ and ~800 locations) | 1999-2000 snapshot | 30 m | N/A | spatial variance, spatial ACF-1, spatial skewness, | Yes (spatial ACF-1) |

| | | | | | | | | | |
|---|---|---|---|---|---|---|---|---|---|
| | | | | | | | | spatial spectra | |
| Congo, Australia | 2019 | [40] | forest-savannah | EVI (MODIS) | 2010 (June-Aug) | 250 m | N/A | spatial var., spatial ACF-1 | Yes (spatial ACF-1) |
| Ireland | 2020 | [20] | pastures | EVI (MODIS) | 2003-2019 | 1 km | 48 d (8 d) | event size/ recovery time | Problematic |
| Amazon basin | in press | [64] | rainforest | VOD (VODCA), NDVI (AVHRR) | 1988-2016 | 0.25° | 1 mth | AR(1), variance | Yes (AR(1)) |
| **Eco-system** | | | | | | | | | |
| N Italy | 2006 | [53] | forest (5 pixels), *fire* | NDVI (SPOT-VEG.) | 1998-2003 | 1 km | 10 d | DFA | Yes |
| Nether-lands | 2017 | [31] | tidal marsh (2 sites), *inundation* | Aerial photos, NDVI | 1976-2012 | 0.25 m | 1 y | recovery rate, spatial variance, spatial correlation | Yes (recovery rate) |
| California | 2019 | [88] | forests | NDVI (Landsat 7) | 1999-2015 | 30 m | 16 d | Bayesian DLM AR(1) | Yes |
| UK | 2021 | [17] | peatland, *drought* | SAR (Sentinel-1) | 2018-2019 | 10 m | 12 d | recovery time | Not really |
| UK | 2021 | [18] | peatland, *management, fires* | dNBR, NDVI (Sentinel-2) | 2016-2020 | 10 m | 2-3 d | recovery time | Not really |
| Sahel | 2021 | [42] | patterned vegetation (40 sites) | NDVI, 'Offset50' (Sentinel-2) | 2016-2019 | 10 m | 1 mth (2 d) | recovery rate, AR(1), variance | Yes |
| Sudan | pre-print | [89] | patterned vegetation | EVI (MODIS) | 2001-2016 | 400 m | 1 mth | AR(1), variance, sensitivity, spatial skewness | Yes (AR(1)) |

*Note: at the equator for longitude and for latitude anywhere 0.1° = 11.1 km.

Abbreviations: NDVI = Normalised Difference Vegetation Index; GPP = Gross Primary Productivity; LAI = Leaf Area Index; VOD = Vegetation Optical Depth; EVI = Enhanced Vegetation Index; SAR = Synthetic Aperture Radar; dNBR = difference Normalised Burn Ratio; DLM = Dynamic Linear Model

# Figures

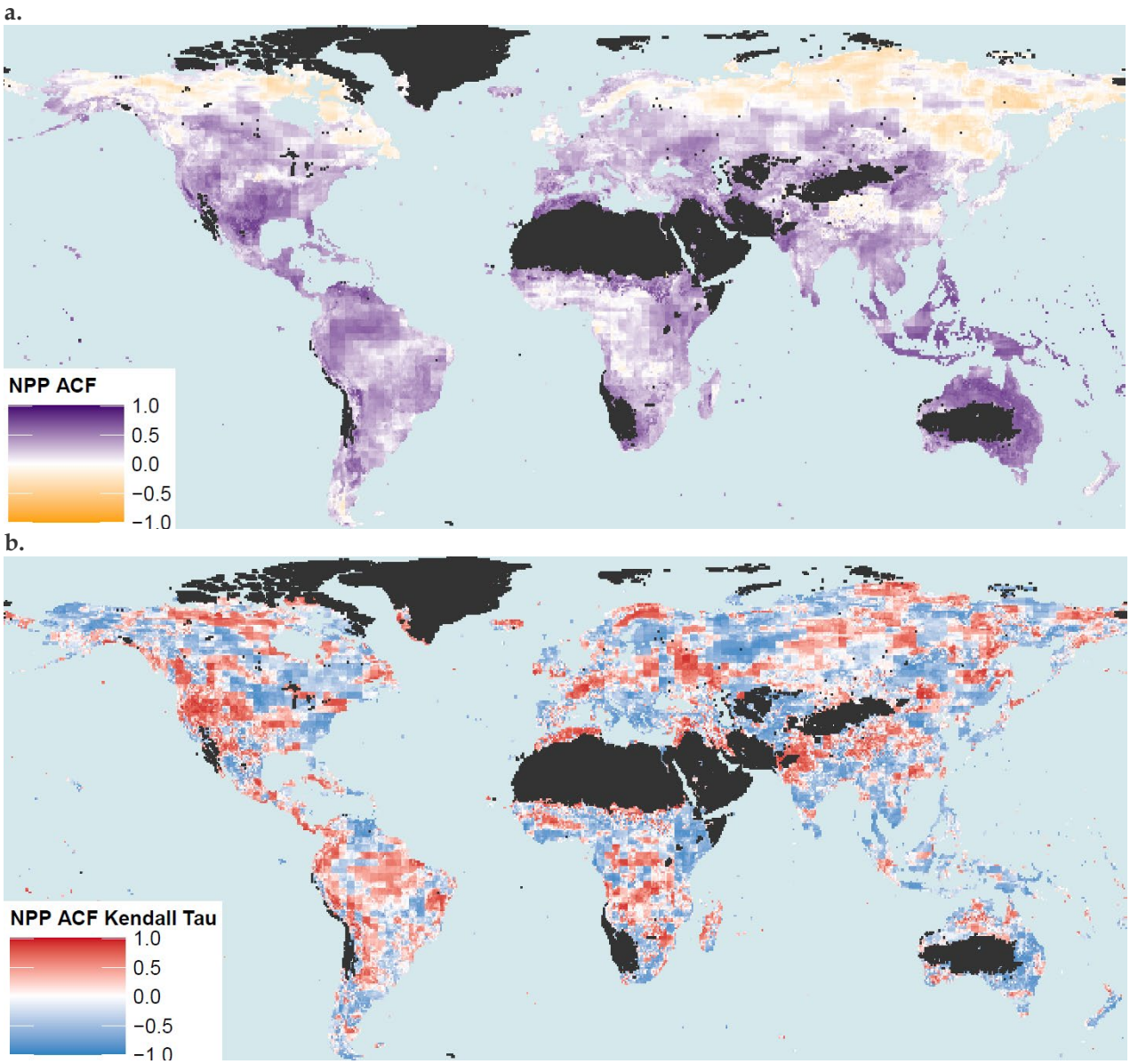


**Figure 1.** Global maps of modelled vegetation resilience: **a.** Autocorrelation function (ACF, equivalent to AR(1)) of modelled monthly NPP (2000-2019) from the LPJmL global vegetation model forced with bias-corrected climate input from the GFDL-ESM2M climate model, where high ACF (AR(1)) corresponds to low resilience (and *vice versa*), and negative ACF (AR(1)) suggests poor fit of an autoregressive model. **b.** Trend in ACF (AR(1)) of monthly NPP (2000-2019) from the same model scenario, measured as Kendall τ rank correlation coefficient, using a 10-year sliding window. Prior to analysis, data are seasonally detrended at the pixel level (with seasonal and trend decomposition using Loess; 'STL') using the '*bfast*' package in R [100-102]. Regions where NPP $<10^{-9}$ kg $m^{-2}$ $s^{-1}$ are filtered out and shown in dark grey.

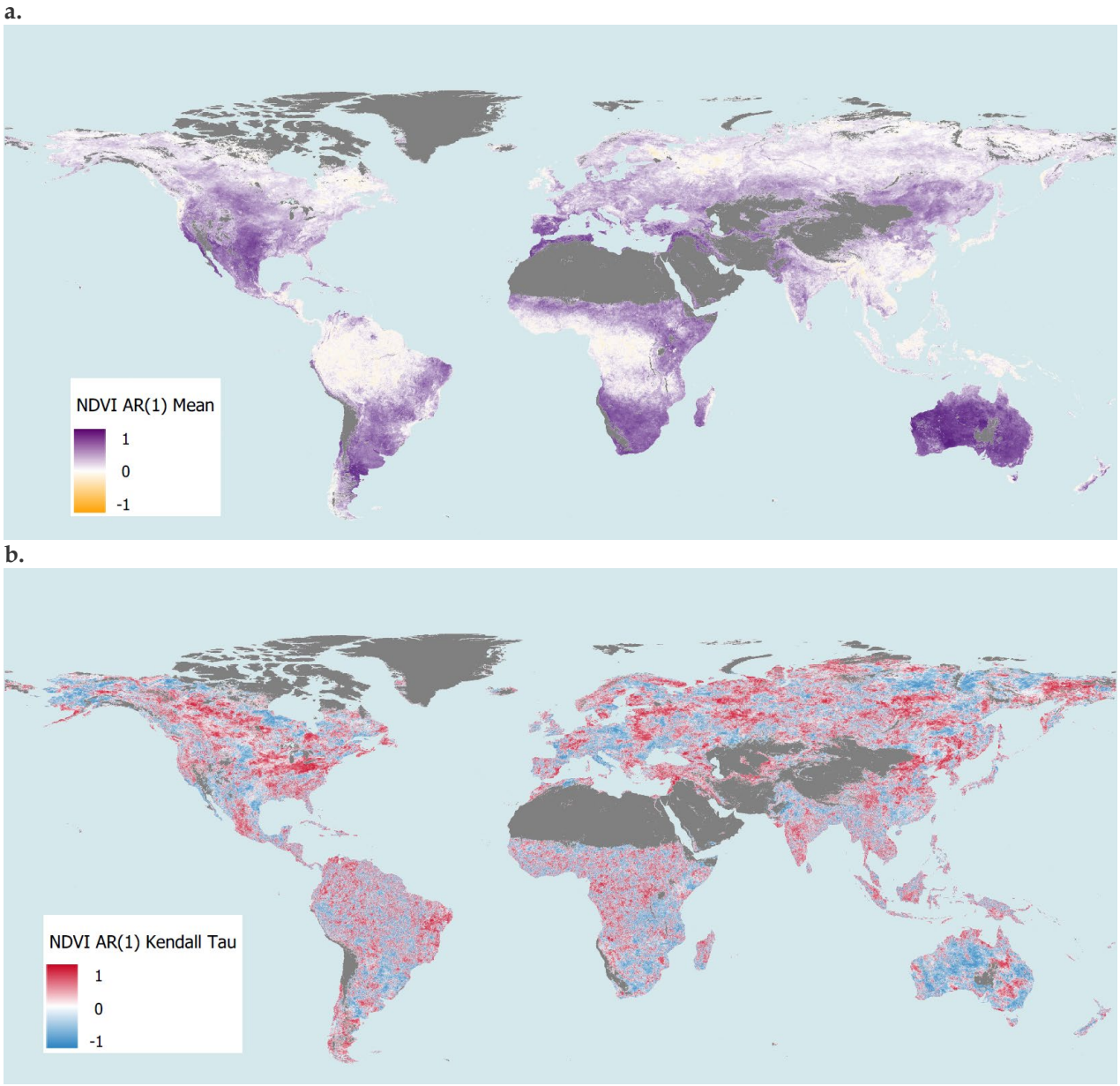


**Figure 2.** Global maps of remotely sensed vegetation resilience: **a.** Mean AR(1) of monthly NDVI (2001-2020 from MODIS), where high AR(1) corresponds to low resilience (and *vice versa*), and negative AR(1) suggests poor fit of an autoregressive model. **b.** Trend in AR(1) (Kendall $\tau$ rank correlation coefficient) of monthly NDVI 2001-2020, using a 10 year sliding window. Prior to analysis, the seasonal cycle is removed by subtracting the 20 year monthly average, then a 25 month moving average is subtracted to remove the trend (a sample of 100 random pixels were analysed to confirm that this seasonal detrending approach gives comparable results to the method used in Figure 1). Regions where NDVI <0.18 are filtered out and shown in grey.

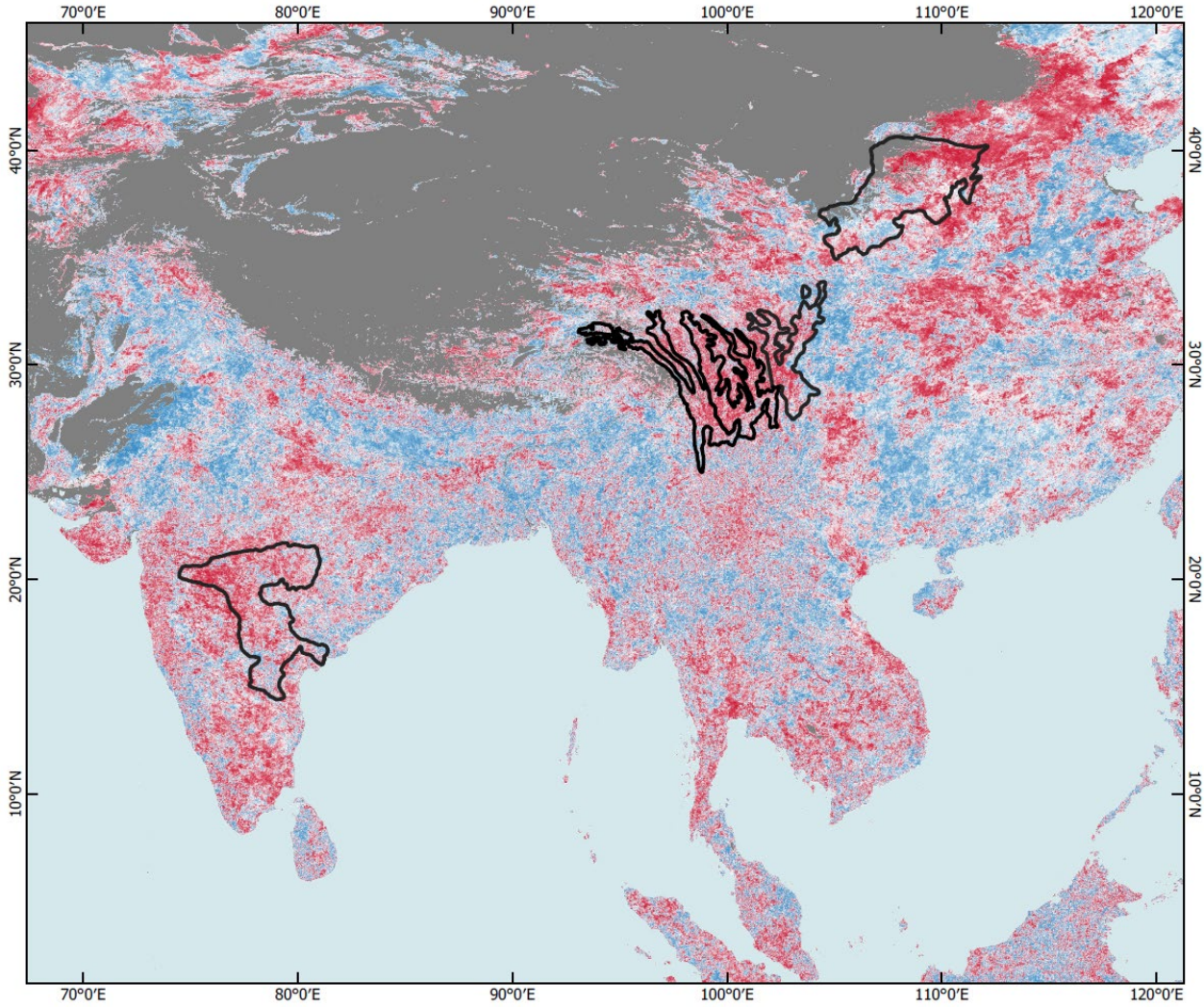


**Figure 3.** Zooming into trends in AR(1) of monthly NDVI (2001-2020) in South and East Asia (from Figure 2b). This shows example ecoregions from the three biomes with globally the most positive AR(1) trends (montane grasslands and shrublands, tropical and subtropical dry broadleaf forests, and temperate coniferous forests). In India, the Central Deccan Plateau dry deciduous forests ($\tau$ =0.67). In Myanmar/China, a group of three coniferous forest ecoregions (west to east): Nujiang Langcang Gorge alpine conifer and mixed forests ($\tau$ =0.60), Hengduan Mountains subalpine conifer forests ($\tau$ =0.78), Qionglai-Minshan conifer forests ($\tau$ =0.79). In northern China: Ordos Plateau steppe montane grassland ($\tau$ =0.62). Regions where NDVI <0.18 are filtered out and shown in grey.